

Numerical Analysis of Heat Transfer Characteristics of an Orthogonal and Obliquely Impinging Air Jet on a Flat Plate

Alenezi A., Teixeira J., and Addali A.

Abstract— This research paper investigates the surface heat transfer characteristics using computational fluid dynamics for orthogonal and inclined impinging jet. A jet Reynolds number Re of 10,000, jet-to- plate spacing (H/D) of two and eight and two angles of impingement (α) of 45° and 90° (orthogonal) were employed in this study. An unconfined jet impinges steadily a constant temperature flat surface using air as working fluid. The numerical investigation is validated with an experimental study. This numerical study employs grid dependency investigation and four different types of turbulence models including the transition SSD to accurately predict the second local maximum in Nusselt number. A full analysis of the effect of both turbulence models and mesh size is reported. Numerical values showed excellent agreement with the experimental data for the case of orthogonal impingement. For the case of $H/D = 6$ and $\alpha = 45^\circ$ a maximum percentage error of approximately 8.8% occurs of local Nusselt number at stagnation point. Experimental and numerical correlations are presented for four different cases.

Index Terms— turbulence model, Inclined jet impingement, single jet impingement, heat transfer

I. INTRODUCTION

The jet Impingement cooling is a complex technique that was introduced to gas turbine blade cooling in the early 1960's and proven to be the most effective technique to improve the heat transfer rate compared to other cooling techniques. It is applied mostly on the inner surface of the blade through small holes in the inner twisted passages to directly impinge hot regions. The jet impingement heat transfer rate from or to a surface depends on several parameters such as: Reynolds number (Re), jet-to-target distance (H/D), jet geometry, turbulence model, target surface roughness and jet temperature as indicated by [1] which will be presented next in detail.

In an orthogonal air jet impinging a flat surface, the flow experiences three regions as shown in Fig. 1

Free jet region: the potential core zone usually exits on a vertical distance of 1.5 jet diameter or more above the target surface. This region contains the potential core zone where the flow has a constant velocity and low level of turbulence intensity. A shear layer starts to develop between the ambient flow and the potential core with high turbulence and lower

mean velocity compared to jet exit velocity. The length of the potential core was investigated by Ashforth-Frost [2] who briefly indicated that by the use of fully developed flow, the potential core length can be elongated by 7% for unconfined jets and 20% for semi-confined jets, this is due the existence of high shear layer. The flow is then fully established at the end of core zone forcing the shear layer to spread and penetrate to the jet centerline. A noticeable increasing in the turbulence intensity beside a decrease in centerline velocity occurs in this region [3].

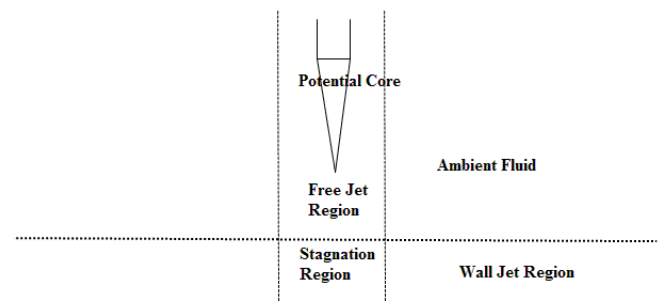


Fig 1 Flow regions of typical single jet impingement

Stagnation region: includes the stagnation point where the mean velocity is zero when the flow stagnates the moment it impinges the surface. Then the flow velocity starts to increase and change its direction from radial to axial. This axial velocity then will be reduced due to the exchange of its momentum with the momentum of the ambient fluid as the distance from the stagnation point increases. The static pressure is approximately equals to the atmospheric pressure due to the variance difference between this region and the ambient region [4].

Wall jet region: wall jet zone where the local flow velocity starts to increase rapidly to a maximum value and then starts to decrease as the distance from the wall increases. This is due to a turbulence generated between the interaction of wall jet and the ambient air

shear [5]. A number of studies have been made propose with different methods to calculate the velocity profiles along this surface as this surface because of the similarity between this surface and the pressure side surface of the turbine blade.

Viskanta [7] performed an experimental study investigating how different jet-to-target distance affects the Nusselt

Manuscript received April 17, 2015; revised April 19, 2014. This work was supported in part by the Kuwait culture office .

A. Alenezi. is with the Cranfield University, Cranfield, Bedfordshire MK43 0AL. UK(phone+4412347501111;e-mail: a.alenezi@cranfield.ac.uk

J. T. is with Cranfield University, Cranfield, Bedfordshire MK43 0AL. UK .(j.a.amaral.teixeira@cranfield.ac.uk)

A.A.is with the Mechanical Engineering Department, , Cranfield, Bedfordshire MK430AL.UK(phone+4412347501111 (a.addali@cranfield.ac.uk)

number using a single 0.78 mm in diameter round jet with Re of 23,000 using different (H/D) . In general, stagnation point has the highest heat transfer coefficient as also indicated by [5]. This observation agreed with results reported from [8] and [9]. A typical (H/D) value of modern gas turbines differs between 1 to 3 [3]. Goldstein and Behbahani [10] reported that a reduction in heat transfer coefficient peak occurs under the influence of cross flow and large jet-to-target distance while at small distances cross flow increases this peak. A secondary peak was also explained by [11] and [12] as an increase in local heat transfer coefficient at low jet-to-target distance at the transition phase between laminar and turbulent flow in wall jet region. This is due the existence of recirculation region as also supported by the sub-atmospheric pressure data [13].

Sagot [14] investigated experimentally the influence of different jet-to-target distances on the average heat transfer coefficient using rounded jet nozzle with diameters range from 2.4 to 8mm. The jet flow temperature ranges between 40 and 65°C impinging a smooth aluminium flat plate which was exposed to a fixed temperature of 4°C under the influence of different Reynolds numbers between 15,000 and 30,000. The author reported that, for large jet-to-target distance ($2 < H/D < 6$), the parameter (H/D) has a weak impact on the average heat transfer coefficient. Miao [15] employed a confined rounded jet array impinging orthogonally a flat plate at different cross flow orientations. He reported that the area-averaged Nusselt number increases by increasing jet-to-target spacing and increasing Reynolds number.

Donaldson [16; 17] made a two-part experimental study of an adjustable axisymmetric jet impinging several surfaces. Jet-to-target distances varied between 1.96 and 39.1 jet diameters with jet angle between 30 and 75° and 1.25 to 6.75 pressure ratios employing sonic and subsonic jets. Hot wire and pressure taps were used to measure surface static pressure and free jet velocity respectively. He conducted that, for $H/D > 20$, the maximum pressure point located on the target surface is a function of impingement angle and the jet pressure ratio almost has no effect. On the other hand, for closer H/D , the strong relation between the maximum pressure ratio location and jet angle still exists but the pressure ratio turned up to be a significant factor. Yan and Saniei [18] used an oblique circular jet impinging a flat plate with angles varied between 45° and 90° to investigate the heat transfer characteristics. Temperature distributions over the preheated plate was measured using transient liquid crystal technique adopting Reynolds numbers between 10,000 and 23,000 and for (H/D) of 4, 7, and 10. Results reported that the point where the maximum heat transfer occurs is shifted away from the geometrical point in the direction of the uphill side of the plate.

Tong [19] in his study investigated numerically the hydrodynamics and heat transfer rate of an inclined plane jet. The results show that with uniform flow profile, the magnitude of the Nusselt number peak increases as increasing the jet angle from normal position. This peak initially declines and then start to rise having a parabolic jet flow profile. His experimental study used an inclined slot jet impinging liquid on a flat plate to investigate the heat transfer from a distance of three jet diameter ($D = 2\text{mm}$) with jet

angles of 45°, 60°, 75°, and 90°. Three low Reynolds number were used of 2500, 5000 and 10,000. He also reported that, beyond jet-to-target distance (H/D) of 3, there is no more change in the hydrodynamics heat transfer as shown in Fig.23. This observation was also reported by the old theoretical study of Miyazaki [20].

In this research paper, a numerical investigation employing ANSYS CFD 14.5 code is adapted to study the effect of jet inclination and jet-to-target distance on the rate of heat transfer on a flat plate. A Reynolds number of 10,000, a normalized jet-to-target distance (H/D) of 2 and 8 and finally two jet inclination angles of (α) of 45° and 90° were employed in this study. A validation of this numerical study was made with the experimental data reported from [21].

II. NUMERICAL METHODOLOGY

The commercial tool Ansys Fluent 14.5 was employed in this study to simulate the jet impingement. Extra attention was taken on the near-wall region since it plays an important role for convective heat transfer. This paper aims to improve the accuracy of the previous numerical studies of jet impingement heat transfer by accurately resolve the near-wall boundary layers of the flow. A validation was made by comparing the results of Nusselt number with experimental results reported by [21].

A. THE COMPUTATIONAL DOMAIN

Half of the actual computational domain was employed since a rounded jet was used as shown in fig.2 in order to save computational cost and time. Fig.2 shows the three dimensional axisymmetric geometry and boundary conditions. Four geometries were studied (table 1). jet-to-target distance H/D was 2 and 8. Angle of impingement α was 45 and 90 (normal impingement). Diameter of inlet pipe was 0.00135 m. For inlet boundary, fully developed pipe flow was calculated using the appropriate RANS model and the profiles of velocity, and turbulence quantities are specified on the inlet boundary. Temperature of inlet flow was 20°C°. Pipe wall was adiabatic. Constant temperature $T_{\text{wall}} = 60\text{C}^\circ$ was supplied to the plate surface. Atmospheric pressure was set in outlet boundaries.

III. GEOMETRY AND BOUNDARY CONDITION

All simulations have been carried out with the use of ANSYS Fluent 14.0 CFD code. The SIMPLEC method is used for pressure and velocity. The inviscid fluxes in the momentum equations are approximated by the use of the second order upwind scheme, the "Standard" interpolation (weighted interpolation based on central coefficients) is utilized and the gradients are approximated using cell based Green-Gauss theorem.

A 2D model of fluid flow and heat transfer coefficient over a backward-facing step is demonstrate. Separating of Boundary layers followed by reattaching occur when applying a uniform heat-flux behind the sudden expansion which distracts local heat transfer figure 4. An experimental data of measured local Nusselt number over the wall are used to validate the current CFD results. A non-uniform Cartesian

mesh sizing 121X61 was adopted in this simulation. A fully developed, steady and incompressible flow with constant properties were used as inlet boundary conditions. The thickness of the incoming boundary layer is 1.1H Figure 1a. Employing the standard wall functions RNG k-ε turbulent model to account for turbulence behavior with Reynolds number $Re=28,000$.

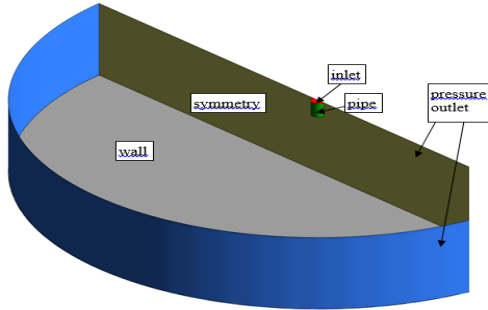


Fig 2 Geometry and boundary conditions

TABLE I PARAMETERS OF GEOMETRY

case	H/D	α , °
1	6	90
2	6	45
3	2	90
4	2	45

A. MESH GENERATION:

In order to resolve the flow features for different H/D and jet angles, a very fine hexahedral mesh was employed in this simulation using grid refinement inside the wall boundary layer. The used mesh is intended to accurately determine the flow parameters as a function of the simulation parameters, grid refinement for boundary layers neighboring the wall is a suitable approach to be use. Generating and then modifying the hexahedral mesh topology to ensure domain orthogonality by first using a course mesh scheme then modifying the mesh to control on the physics distance of the first node from the wall (y^+). Keeping the y^+ equals or below 0.5 for the near-wall cells is an important step to resolve the viscous laminar sublayer which needs at least 12 nodes. The final mesh is designed to have nodes near the target surface where jet mixing occurs.

Grid independence was investigated for case 1 ($H/D = 6$) where three grids were generated as shown in table 2 using ANSYS ICEM CFD 14.5 code.

TABLE II GRID EMPLOYED

No	Size, cells	Y^+
1	400 000	0.5
2	986 000	0.5
3	1 783 000	0.5

The Maximum aspect ratio for all grids is 1.15, and the height of the first node from the wall was about 0.005mm for all grids. Giving a y^+ value ≤ 0.5 for the whole wall surface. In addition, approximately about 12 nodes are applied within the viscous laminar sublayer for small distances to ensure a full resolve of this critical thin layer. Figure 3 shows base grid of grid no.2

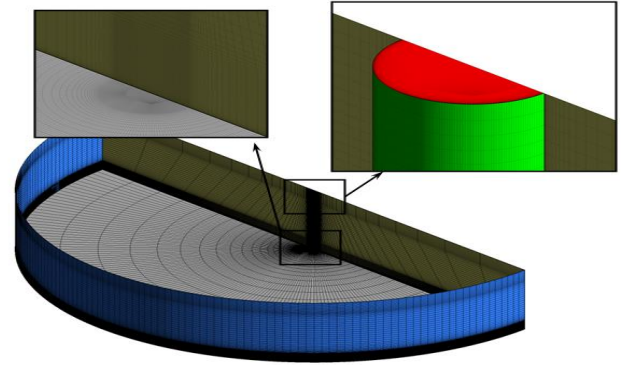


Fig 3 Mesh Generation of grid no2

B. FLUID PROPERTIES:

Air at 25°C is adopted as the coolant flow assuming an incompressible flow since the Mach number is less than 0.05. Air viscosity μ and density ρ are assumed to be constant with values of $= 1.79e-5$ kg/m.s and 1.225 kg/m³. Reynolds number of a fixed value of 10,000 was calculated based on the jet hydraulic diameter ($D_h = 0.0135$) using the equation ($Re = U_{ref} D_h \rho / \mu$) giving a U_{ref} equals 10.8 m/s. The Nusselt number is obtained using the equation ($Nu = Q D_h / ((T_{jet} - T_{wall}) * K)$) where the jet temperature T_{jet} and air thermal conductivity are 25°C and 0.0242 W/m.k. respectively.

C. TURBULENCE MODELLING

Although the geometry of the jet impingement considered to be relatively simple but the flow physics is very complicated within the different impingement zones. The flow jet velocity reached zero at the stagnation point where maximum static pressure occurs and then starts to increase radially in both direction creating laminar, transition and turbulent flow regions. All these regions should be considered in order to solve the energy equation in high level of accuracy. In order to decide which turbulence model to use, both flow physics and computational requirements should be well known. It is not recommended to use the wall function due to the separation in the boundary layer near the wall [22]. Therefore; a very fine mesh needs to be generated near the wall with a y^+ value ≤ 0.5 to include the thin laminar boundary layer so the results will be accurate. The turbulence models considered in this study are: k-ε with enhanced wall function, transition SST, shear stress transport (SST-trans) and Reynolds stress (RSM).

D. SOLUTION APPROACH

The SIMPLEC scheme and Green-Gauss Cell Based gradient for spatial discretization were employed in this study using second order discretization schemes energy and momentum equations to produce more accurate results for heat transfer where first order schemes were used for other equations. Several steps were used before finalizing the solution: first, the use of the entire domain initialized by the inlet flow conditions employing first order upwind discretization to reach a convergence criteria at 10^{-6} for energy equation and 10^{-4} for the rest. The second step is seeking the solution by mixing up different orders of discretization schemes.

IV. SENSITIVITY ANALYSIS

The next sub-sections introduce an inclusive analysis of both models and parameters when employing the numerical model. An intensive discussion in each sub-section is carried out for CFD mythology aspect and validated with experimental data in [21]. For clarification, only one comparison to the experimental data was performed employing k-ε turbulence model, Re=10,000, α=90° and H/D=6 to specify the appropriate grid size to use for the rest of simulations. In all following figures, experimental data are signified by line with triangles marks. The effects of jet angles (α) and jet-to-target distances (H/D) on the heat transfer rate will be discussed in section 4.

A. DISCRETIZATION SCHEME

To increase the results accuracy of heat convection in jet impingement, a higher order discretization scheme must be adapted. A succeeding enhancement from the first to second order discretization scheme improves the numerical heat transfer rate compared to the experimental values. In order to capture the secondary peak in Nusselt number (Nu) distribution which occurs at a certain radial distance from the stagnation point, a second order scheme should be employed on the domain. The first order scheme however, is not consistent with the experimental data for short radial distance r/D < 2 where the laminar-turbulence transition region occurs.

B. GRID REFINEMENT STUDY

A grid analysis is employed in this study to certify that the solution is independent of the computational grid. Generally, both numerical solution accuracy and numerical time depend mainly on mesh refinement. In this work, the suitable grid is examined to have the proper run-time and accuracy. Three grid cases considered in the present grid refinement study, as shown in table 2. Figure 4 shows values of Nusselt number varied with the radial distance r/D under the influence of k-ε turbulence model, H/D=6 and jet angle of 90° for different grids. It is notable, that both experimental and the numerical local Nusselt number values are close for all grid cases and therefore, grid 2 will be used for the rest of the numerical cases.

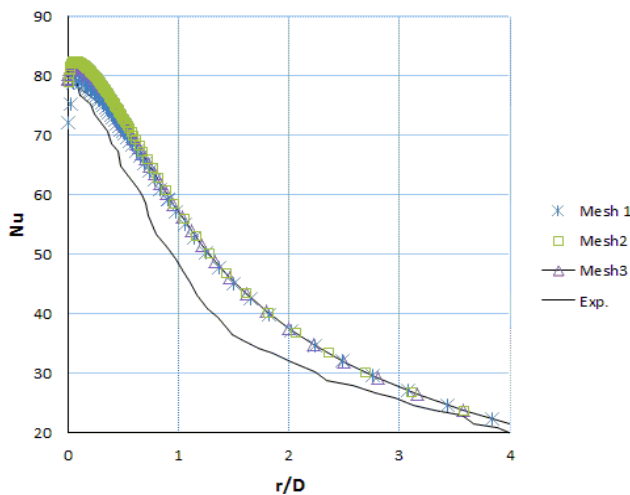


Fig 4 Nusselt number distribution for three types of grids

C. CODE VALIDATION

To validate the numerical results, the local Nusselt number Nu is compared to the benchmark experimental data by O'Donovan and Murray [21] for four different turbulence models. Comparison between results is shown in figure 5. As shown in this figure, for an orthogonal jet with H/D=6, the k-ε turbulence model shows an excellent agreement with the experimental data comparing to the other three turbulence models. Therefore, the k-ε turbulence model will be used for all simulation cases.

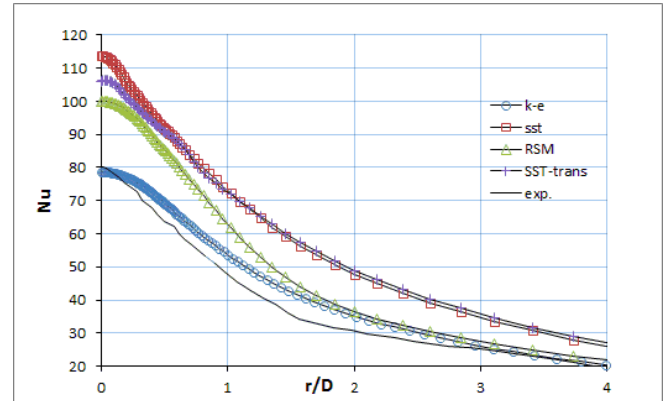


Fig 5 Local Nusselt number Vs r/D for four different turbulence models

V. RESULTS AND DISCUSSION

In this study, varies jet-to-target spacing and jet inclination angles were employed to study their effect on the convection heat transfer rate. The Reynolds number was fixed to 10,000 for both case of H/D=6 and H/D=2. The modelling results were obtained using the k-ε turbulence model and grid 2 case. Figure 6 shows the values of local Nusselt numbers Nu for jet inclination angles of 90° and 45° in the case of jet-to-target spacing (H/D) equals six. For orthogonal spacing (H/D) equals six. For orthogonal impingement (α=90°), an excellent agreement between the numerical and experimental value of Nu local maxima which occurs at the stagnation point with a bit higher values as the radial distance increases. However, In the case of inclined jet angle (α=45°), the numerical result shows less local maxima Nu than the experimental value. This could be due to the high turbulence intensity and shear layer mixing between jet flow and the surrounded flow at the jet nozzle exit. A higher numerical Nu values are shown for the rest of the impinging plate in the case of inclination jet.

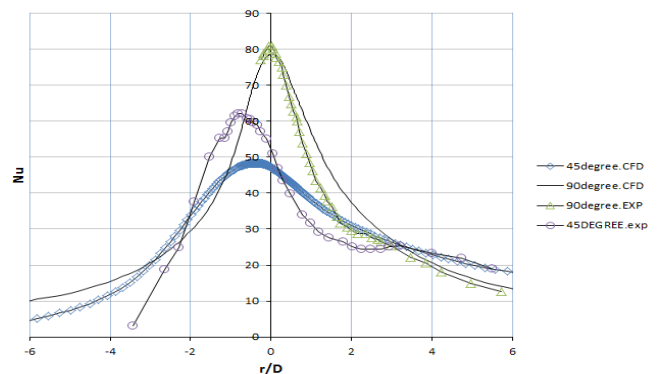


Fig 6 Local Nusselt number for different jet angles at H/D=6.

Figure 7 illustrates the same study discussed in the last paragraph but for a closer jet-to-target spacing ($H/D=2$). It is noticeable that the overall values of local Nusselt numbers for both numerical and experimental increase by decreasing the jet-to-target spacing due to less turbulence intensity and higher jet arrival velocity. For orthogonal jet, the numerical local Nusselt number values show higher in magnitude than the experimental values for all radial distances except for $r/D \geq 2$ where both values become to be much closer. This is not the case for the inclination jet, where the experimental values of local Nusselt number are higher at the stagnation point and then become lower for the rest of the radial distances

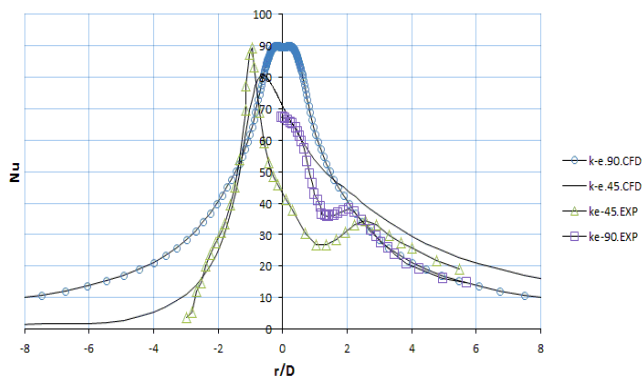


Fig 7 Local Nusselt number for different angles at $H/D=2$

Figures 8a and 8b show the velocity magnitude distributions of the orthogonal jet for $H/D=6$ and $H/D=2$ respectively. Comparing the value of the arrival velocity for both cases, it can be noticed that as the H/D increases, the arrival jet velocity decreases and the turbulence intensity increases

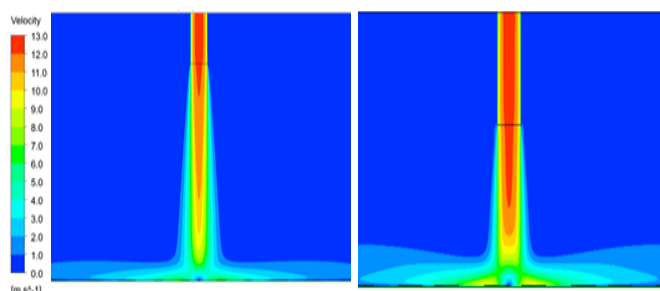


Fig 8 Velocity distributions of orthogonal jet for a) $H/D=6$, b) $H/D=2$

Figures 9 a and b show the velocity magnitude distribution of a jet angle ($\alpha=45^\circ$) where the stagnation point is different from the geometric center. The arrival jet velocity in the case of lower jet-to-target spacing is higher in magnitude than it is in the case of higher jet-to-target spacing. On the other hand, the turbulence intensity is lower for lower H/D .

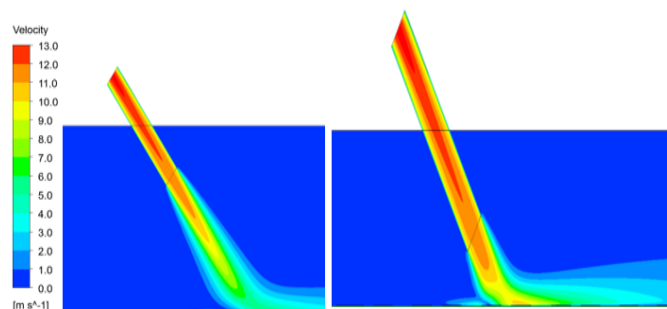


Fig 9 Velocity distributions of inclined jet for a) $H/D=6$, b) $H/D=2$

VI. CONCLUSION

The use of $k-\epsilon$ turbulence model saves computational time and cost with accurate results in prediction the heat transfer rate when compared to the detailed experimental results for validation. Furthermore, all physics properties of both the jet and the heated plate accurately calculated by adapting grid density in the near-wall region. Results reported from this study were captured using $Re=10,000$, jet-to-target spacing H/D between two and six. The values of the dimensionless distance between the wall and the first node (y^+) and Prandtl number in the near-wall region have proven to be important parameters in predicting the turbulent heat transfer since their values effect directly the heat diffusion level. Interestingly enough that all the four turbulent models used in this study have failed to predict the secondary peak of Nusselt number which supposed to occur at approximately $r/D=3$. Alternative turbulent models such as Large Eddy Simulation (LES) or Detached Eddy Simulation (DES) can be used such in order to predict the Nusselt number secondary peak.

The use of accurate boundary conditions including fluid properties, appropriate computational domain, and the right solution approach has been proven to be the main parameters in order to accurately predict the heat transfer rate for circular jet impingement.

REFERENCES

- [1] Jambunathan, K., Lai, E., Moss, M. A. and Button, B. L. (1992), "A review of heat transfer data for single circular jet impingement", *International Journal of Heat and Fluid Flow*, vol. 13, no. 2, pp. 106-115.
- [2] Ashforth-Frost, S. and Jambunathan, K. (1996), "Effect of nozzle geometry and semi-confinement on the potential core of a turbulent axisymmetric free jet", *International Communications in Heat and Mass Transfer*, vol. 23, pp. 155-162.
- [3] O'Donovan, T. S., and Murray, D. B., 2007, "Jet Impingement Heat Transfer— Part I: Mean and Root-Mean-Square Heat Transfer and Velocity Distributions," B. Smith, "An approach to graphs of linear forms (Unpublished work style)," unpublished.
- [4] Livingood, J., N. B. and Hryack, P. (1973), "impingement heat transfer from turbulent air jets to flat plates", NASA TM X-2778, J.
- [5] Zuckerman, N. and Lior, N. (2005), "Impingement Heat Transfer: Correlations and Numerical Modeling", *Journal of Heat Transfer*, vol. 127, no. 5, pp. 544-552.
- [6] Donaldson, C. D., and Snedeker, R. S., 1971, "A study of free jet impingement, part I mean properties of free impinging jets," *Journal of Fluid Mechanics*, 45, pp. 281-319.
- [7] Viskanta, R. (1993), "Heat Transfer to impinging isothermal gas and
- [8] Hollworth, B. R. and Wilson, S. I. (1984), "Entrainment Effects on Impingement Heat Transfer. Part 1 Measurements of Heat Jet Velocity and Temperature Distributions and Recovery Temperatures on Target Surfaces", *J. of Heat Transfer*, vol. 106, pp. 797-803
- [9] Sparrow, E. M. and Lovell, B. J. (1980), "Heat Transfer Characteristics of an Obliquely Impinging Circular Jet", *J. Heat Transfer*, vol. 102, pp. 202-209.
- [10] Goldstein, R. J. and Behbahani, A. I. (1982), "Impingement of a circular jet with and without cross flow", *Int. J. Heat Mass Transfer*, vol. 25, no. 9, pp. 1377-1382.

- [11] Lytle, D. and Webb, B. W. (1994), "Air jet impingement heat transfer at low nozzle-plate spacings", *Int. J. Heat Mass Transfer*, no. 12, pp. 1687-1697.
- [12] Walker, D. A. and Smith, C. R. (1987), "The impact of a vortex ring on a wall", *J. Fluid Mech.*, vol. 181, pp. 99-140.
- [13] Colucci, D. W. and Viskanta, R. (1996), "Effect of nozzle geometry on local convective heat transfer to a confined impinging air jet", *Experimental Thermal and Fluid Science*, vol. 13, no. 1, pp. 71-80.
- [14] Sagot, B., Antonini, G., Christgen, a. and Buron, F. (2008), "Jet Impingement heat transfer on a flat plate at a constant wall temperature", *International Journal of Thermal Sciences*, vol. 47, no. 12, pp. 1610-1619.
- [15] W. Lucky, "Automatic equalization for digital communication," *Bell Syst. Tech. J.*, vol. 44, no. 4, pp. 547-588, Apr. 1965.
- [16] R. Faulhaber, "Design of service systems with priority reservation," in *Conf. Rec. 1995 IEEE Int. Conf. Communications*, pp. 3-8.
- [17] G. R. Faulhaber, "Radio noise currents n short sections on bundle conductors (Presented Conference Paper style)," presented at the IEEE Summer power Meeting, Dallas, TX, Jun. 22-27, 1990, Paper 90 SM 690-0 PWRS.
- [18] Donaldson, C., Snedeker, R. and Margolis, P. (1971), "A study of jet impingement. Part 2. Free jet turbulent structure and impingement heat transfer", *J. Fluid Mech.*, vol. 45, no. 3, pp. 477-512.
- [19] Donaldson, C. and Snedeker, R. (1971), "A study of free jet Impingement. Part 1. Mean properties of free and impinging jets", *J. Fluid Mech.*, vol. 45, no. 2, pp. 281-319.
- [20] Yan, X. and Saniei, N. (1997), "Heat transfer from an obliquely impinging circular, air jet to a flat plate", *International Journal of Heat and Fluid Flow*, vol. 18, no. 6, pp. 591-599.
- [21] Tong, A. Y. (2003), "On the impingement heat transfer of an oblique free surface plane jet", *International Journal of Heat and Mass Transfer*, vol. 46, no. 11, pp. 2077-2085
- [22] Miyazaki, H. and Silberman, E. (1972), "Flow and heat transfer on a flat plate normal to a two-dimensional laminar jet issuing from a nozzle of finite height", *International Journal of Heat and Mass Transfer*, vol. 15, no. 11, pp. 2097-2107.
- [23] O'Donovan, T. and Murray, D. (2008), "Fluctuating fluid flow and heat transfer of an obliquely impinging air jet" *International Journal of Heat and Mass Transfer* 51 (2008) 6169-6179 pp. 2097-2107.
- [24] Hadziabdic, M., and Hanjalic, K., 2008, "Vortical Structures and Heat Transfer in a Round Impinging Jet," *J. Fluid Mech.*, 596, pp. 221-260
- [25] O'Donovan, 2005, *FLUID FLOW AND HEAT TRANSFER OF AN IMPINGING AIR JET*. PhD thesis, University of Dublin